

1 **First-Principles Study on Structural Properties of GeO₂ and SiO₂**
2 **under Compression and Expansion Pressure**

3 Shoichiro SAITO* and Tomoya ONO

4 *Graduate School of Engineering, Osaka University, 2-1 Yamadaoka, Suita, Osaka 565-*
5 *0871, Japan*

6 (Received)

7 The detailed analysis of the structural variations of three GeO₂ and SiO₂ polymorphs
8 (α -quartz, α -cristobalite, and rutile) under compression and expansion pressure is re-
9 ported. First-principles total-energy calculations reveal that the rutile structure is the
10 most stable phase among the phases of GeO₂, while SiO₂ preferentially forms quartz.
11 GeO₄ tetrahedras of quartz and cristobalite GeO₂ phases at the equilibrium volume are
12 more significantly distorted than those of SiO₂. Moreover, in the case of quartz GeO₂
13 and cristobalite GeO₂, all O-Ge-O bond angles vary when the volume of the GeO₂ bulk
14 changes from the equilibrium point, which causes further deformation of tetrahedra. In
15 contrast, the tilt angle formed by Si-O-Si in SiO₂ markedly changes. This flexibility of
16 the O-Ge-O bonds reduces the stress at the Ge/GeO₂ interface due to the lattice-constant
17 mismatch and results in the low defective interface observed in the experiments [Matsub-
18 ara *et al.*: Appl. Phys. Lett. **93** (2008) 032104; Hosoi *et al.*: Appl. Phys. Lett. **94**
19 (2009) 202112].

20 **KEYWORDS:**

* E-mail address: saito@cp.prec.eng.osaka-u.ac.jp

21 1. Introduction

22 Ge has recently attracted increasing attention for future advanced complementary metal
23 oxide semiconductor (CMOS) device structures owing to its high intrinsic carrier mobil-
24 ity as it is becoming increasingly difficult to enhance the performance of CMOS devices
25 through scaling based on conventional Si-based techniques. The key issue to be resolved in
26 advanced Ge-based devices is the formation of gate stacks with superior interface proper-
27 ties. Research activity related to GeO_2 is steadily increasing, and it has been reported that
28 Ge is well passivated by GeO_2 by conventional dry oxidation without any hydrogen pas-
29 sivation treatment.^{1,2} On the theoretical side, Houssa *et al.* claimed that the viscoelastic
30 properties of GeO_2 lead to a low interface defect density at the Ge/ GeO_2 interface af-
31 ter performing a calculation using a modified Maxwell model.³ In our previous study,
32 we examined the oxidation mechanism of crystalline GeO_2 and Ge(100) interfaces by a
33 first-principles total energy calculation following the Si(100) oxidation process proposed
34 by Kageshima and Shiraishi,⁴ and we found that Ge atom emission, which deteriorates
35 the Ge/ GeO_2 interface, hardly occurs during the oxidation process of Ge(100).⁵ To inves-
36 tigate the low probability of Ge atom emission, the mechanism accounting for the release
37 of interface stress should be clarified.

38 From the viewpoint of phase transition, SiO_2 occurs in many different forms. At ambient
39 temperature and pressure, the ground-state structure for SiO_2 is α -quartz (q- SiO_2). SiO_2
40 forms a rutile structure (r- SiO_2) under a pressure above 2 GPa and it is transformed
41 into α -cristobalite (c- SiO_2) at a high temperature. On the other hand, there are two
42 stable polymorphs of GeO_2 at normal pressures: the low temperature form has the rutile
43 structure (r- GeO_2), and GeO_2 undergoes a smooth transformation to α -quartz (q- GeO_2)
44 at $T \approx 1300$ K. An α -cristobalite structure (c- GeO_2) has been identified after the long-
45 time heating of GeO_2 glass at 873 K.⁶ The investigation of the c- GeO_2 phase is important
46 because Ge substrates are typically subjected to dry oxidation in an O_2 ambient at 623-823
47 K to form a GeO_2 layer in recent experiments.^{2,7}

48 Here, we investigate the structural properties of q-, c-, and r- GeO_2 by first-principles
49 total energy calculations. The structural properties of SiO_2 are also examined for compar-

ison. It was found that the rutile structure of GeO_2 is the most stable structure, whereas SiO_2 preferentially forms the quartz structure. We then investigate the variations of the O-Ge-O (O-Si-O) bond angles of quartz and cristobalite phases with respect to the volume since local pressure is induced at the semiconductor/oxide interface. Although the variations of the atomic structures of q- GeO_2 , r- GeO_2 , q- SiO_2 , c- SiO_2 , and r- SiO_2 under pressure have been examined by both experimental and theoretical studies,⁸⁻²⁰ no study reports the relationship between their bond angles and pressure of these six oxides in the same treatment of computational code or experimental facility. We note that the lattice constant (bulk modulus) of q- SiO_2 reported by the first-principles calculation¹⁵ is smaller (larger) by more than 3 % (34 %) than the one reported by another first-principles study.¹⁶ Moreover, it is reported that a dioxide forms a cristobalite structure before the atom emission as well as at the initial stage of oxidation.⁴ The pressure-dependent behavior of c- GeO_2 , which has never been explored to the best of our knowledge, is a subject of intense research to clarify the relaxation mechanism of the interface stress. Therefore, it is of importance that the uniform theoretical treatment facilitates systematic comparisons and the identification of trends among these six oxides. Our finding is that the O-Ge-O bond angles change significantly under pressure, while the tilt angle and Si-O bond length vary in the case of SiO_2 . The variation of the bonding network of GeO_2 exhibits completely different characteristics from that of SiO_2 . The metallic properties of Ge provide a qualitative understanding of not only the difference between the ground-state phases of GeO_2 and SiO_2 but also the variations of the bond angles under pressure.

The rest of this paper is organized as follows. In § 2, we describe the computational techniques used in this study. In § 3, we present the main results and a discussion of the structural parameters and properties. Finally, a brief summary is given in § 4.

2. Computational Techniques

The structures of q-, c-, and r- GeO_2 are hexagonal, tetragonal, and tetragonal with three, four, and two GeO_2 molecules per unit cell, respectively. Ge atoms in q- and c- GeO_2 are surrounded by four oxygen atoms, while each Ge atom in r- GeO_2 is surrounded by six oxygen atoms with distorted octahedral coordination as shown in Fig. 1. The

79 calculations are performed within the local density approximation²¹ of density functional
 80 theory^{22,23} using the real-space finite-difference approach²⁴⁻²⁸ and the norm-conserving
 81 pseudopotentials²⁹ of Troullier and Martins³⁰ in the Kleinman-Bylander representation.³¹
 82 The grid spacing was set at 0.25 bohr, and a denser grid spacing of 0.083 bohr in the
 83 vicinity of nuclei with the augmentation of double-grid points²⁷ for each GeO₂ polymorph.
 84 We took $4 \times 4 \times 4$, $4 \times 4 \times 3$, and $4 \times 4 \times 6$ k -point grids in the Brillouin zone for q-, c-,
 85 and r-GeO₂, respectively. The optimal lattice parameters and internal atomic coordinates
 86 were determined by minimization of the total energy using calculated forces, with a force
 87 tolerance of $F_{max} < 1.0$ mH/bohr. The same computational procedures were applied for
 88 SiO₂ polymorphs.

89 3. Results and Discussion

90 Figures 2 (a) and (b) show the total energy per molecular unit as a function of volume
 91 for the three structures of GeO₂ and SiO₂, respectively. The zeros of the energy scales
 92 are rutile for GeO₂ and quartz for SiO₂. It was found that the zero-temperature phase in
 93 GeO₂ has the rutile structure while that in SiO₂ exhibits the quartz structure, which is in
 94 good agreement with a previous report.^{18,32} Sn, which is also a group IV element similarly
 95 to Si and Ge, is a metal and its oxide crystallizes in the rutile structure under ambient
 96 conditions.³³ GeO₂ forms the sixfold-coordinated rutile structure more preferentially than
 97 SiO₂ because Ge is between Si and Sn in the periodic table. Tables I and II show the
 98 calculated lattice constants, bond lengths l_i , bond angles θ_j , and tilt angles δ of GeO₂ and
 99 SiO₂. The other calculated and experimental results are also given.^{9,10,20,34-37} There are
 100 two distinct Ge-O (Si-O) bond lengths in GeO₄ (SiO₄) tetrahedra. In addition, θ_j exactly
 101 corresponds to the O-Ge-O (O-Si-O) bond angle, and the tilt angle is related to the Ge-O-
 102 Ge (Si-O-Si) bond angle.^{38,39} The agreement between our results and experimental results
 103 for SiO₂ is excellent for the structural parameters. The lattice constants of q- and c-GeO₂
 104 are slightly underestimated in both the theoretical calculations: this underestimation is
 105 caused by the use of the local density approximation,²¹ and the parameters obtained by
 106 the theoretical calculations agree well. The deviations of the O-Ge-O bond angles from
 107 the ideal tetrahedral angle (109.5°) are larger than those for O-Si-O, resulting in distorted

108 GeO_4 tetrahedra.

109 Thermally oxidized GeO_2 on a Ge substrate has been found to mainly form the fourfold-
110 coordinated structure by X-ray photoelectron spectroscopy,⁴⁰ and crystalline q- and c-
111 SiO_2 are formed on a Si(100) surface according to the oxidation model of the Si(100)
112 surface.⁴ The compressive in-plane stress at the Ge/ GeO_2 (Si/ SiO_2) interface is induced
113 by the lattice mismatch between Ge (Si) and its oxide. Therefore, we particularly focus on
114 the bond structures of crystalline q- and c- GeO_2 assuming that the oxidation mechanism
115 of Ge is the same as that of Si. Figures 3, 4, and 5 show the variations of the Ge-O
116 (Si-O) bond lengths, the O-Ge-O (O-Si-O) bond angles, and the tilt angles with respect
117 to the volume, respectively. In the case of the rutile phases, we depict the variations of
118 the Ge-O-Ge (Si-O-Si) bond angles instead of the tilt angles since the rutile structure has
119 a higher symmetry than the others. The models at elevated pressures do not exhibit the
120 amorphous phase or transform into another phase because the calculated O-Ge-O and
121 O-Si-O bond angles show no indication that the tetrahedra become significantly more
122 irregular or distorted. Although the lattice constants are varied by increments of 1%,
123 the variations of the bond lengths are less than $\sim 0.1\%$. This indicates that the bond
124 angles play a predominant role in the compression or expansion of the fourfold oxides.
125 Note that the bond lengths in the sixfold oxides change under pressure due to the higher
126 symmetry of the O-Ge-O (O-Si-O) bond angles as well as the Ge-O-Ge (Si-O-Si) ones.
127 The variations of the O-Ge-O bond angles are larger than those of O-Si-O [Figs. 4(a)
128 and 4(b)], whereas the tilt angles in SiO_2 vary more significantly than those in GeO_2
129 [Figs. 5(a) and 5(b)] with respect to the volume. These results indicate the strong
130 rigidity of the O-Si-O bonds. The experimental study reported that the O-Ge-O bond
131 angles markedly change in q- GeO_2 , while the tilt angle in q- SiO_2 varies significantly as
132 the pressure increases, which agrees well with our result.⁸ The metallic property of Ge,
133 as mentioned above, is also attributed to the distorted GeO_4 tetrahedra and the variation
134 of the O-Ge-O bond angles from the ideal tetrahedral angle. This characteristic of the O-
135 Ge-O bonds leads to markedly reduced lattice stress at the Ge/ GeO_2 interface during the
136 oxidation process compared with its Si counterpart. Kageshima and Shiraishi reported
137 that SiO_2 forms a cristobalite structure at the initial stage of Si oxidation transforms into

138 a quartz structure after the Si atom at the Si/SiO₂ interface has been ejected to release
139 the interface stress.⁴ We also investigated the emission of Ge atoms from the Ge/c-GeO₂
140 interface following their model and found that Ge atoms are hardly emitted.⁵ We have
141 concluded that this is because the dispersion of the bond angles around the suboxidized
142 Ge atom at the Ge/GeO₂ interface is larger than that around the Si atom at the Si/SiO₂
143 interface. The present result that the bond angles around Ge atoms in c-GeO₂ also more
144 drastically change than those around Si atoms as well as those in the other phases supports
145 the conclusion in our preceding study.

146 4. Conclusions

147 We have calculated the bond lengths and bond angles of the rutile, α -cristobalite, and
148 α -quartz phases of GeO₂ and SiO₂ using first-principles electronic-structure calculations.
149 It was found that rutile GeO₂ is the most stable phase among the structures of GeO₂
150 examined here while SiO₂ preferentially forms the quartz structure, which agrees well
151 with previous first-principles results. Symmetry allows four different O-Ge-O (O-Si-O)
152 tetrahedral angles in GeO₄ (SiO₄) in the case of the cristobalite and quartz phases, and
153 the angles in GeO₄ are more distorted from the ideal tetrahedral angle (109.5°) than those
154 in SiO₄ at the equilibrium volume. Moreover, we have also examined the variation of the
155 bond lengths and bond angles with respect to volume and found that the mechanisms
156 leading to compression and expansion are markedly different between GeO₂ and SiO₂
157 even though the volume compressibilities and expansibilities are almost identical: the
158 tetrahedra of GeO₄ are significantly deformed under pressure whereas the tilting angle
159 composed of two tetrahedras markedly varies in the case of SiO₂. These characteristics of
160 GeO₂, i.e., the ground-state phase of the oxides and the difference in the variation of bond
161 angles with respect to the volume, can be interpreted in terms of the metallic properties
162 of the bond network of Ge. Thus, our results are highly relevant to the low defect density
163 at the Ge/GeO₂ interface because the deterioration of the interface is suppressed owing
164 to the flexibility of the O-Ge-O bond angles.

165 **Acknowledgements**

166 The authors would like to thank Professor Kikuji Hirose, Professor Yoshitada Morikawa,
167 and Professor Heiji Watanabe of Osaka University, and Professor Kenji Shiraishi of Uni-
168 versity of Tsukuba for reading the manuscript and fruitful discussions. This research
169 was partially supported by Strategic Japanese-German Cooperative Program from Japan
170 Science and Technology Agency and Deutsche Forschungsgemeinschaft, by a Grant-in-
171 Aid for Young Scientists B (No. 20710078), and also by a Grant-in-Aid for the Global
172 COE "Center of Excellence for Atomically Controlled Fabrication Technology" from the
173 Ministry of Education, Culture, Sports, Science and Technology, Japan. The numerical
174 calculation was carried out using the computer facilities of the Institute for Solid State
175 Physics at the University of Tokyo, Center for Computational Sciences at University of
176 Tsukuba, the Research Center for Computational Science at the National Institute of
177 Natural Science, and the Information Synergy Center at Tohoku University.

178 **References**

- 179 1) H. Matsubara, T. Sasada, M. Takenaka, and S. Takagi: Appl. Phys. Lett. **93** (2008)
180 032104.
- 181 2) T. Hosoi, K. Kutsuki, G. Okamoto, M. Saito, T. Shimura, and H. Watanabe: Appl.
182 Phys. Lett. **94** (2009) 202112.
- 183 3) M. Houssa, G. Pourtois, M. Caymax, M. Meuris, M. M. Heyns, V. V. Afanas'ev, and
184 A. Stesmans: Appl. Phys. Lett. **93** (2008) 161909.
- 185 4) H. Kageshima and K. Shiraishi: Phys. Rev. Lett. **81** (1998) 5936.
- 186 5) S. Saito, T. Hosoi, H. Watanabe, and T. Ono: Appl. Phys. Lett. **95** (2009) 011908.
- 187 6) H. Böhm: Naturwissenschaften **55** (1968) 648.
- 188 7) A. Delabie, F. Bellenger, M. Houssa, T. Conard, S. Van Elshocht, M. Caymax, M.
189 Heyns, and M. Meuris: Appl. Phys. Lett. **91** (2007) 082904.
- 190 8) J. D. Jorgensen: J. Appl. Phys. **49** (1978) 5473.
- 191 9) L. Levien, C. T. Prewitt, and D. J. Weidner: Am. Mineral. **65** (1980) 920.
- 192 10) R. T. Downs and D. C. Palmer: Am. Mineral. **79** (1994) 9.
- 193 11) V. P. Prakapenka, G. Shen, L. S. Dubrovinsky, M. L. Rivers, and S. R. Sutton: J.
194 Phys. Chem. Solids **65** (2004) 1537.
- 195 12) M. Vaccari, G. Aquilanti, S. Pascarelli, and O. Mathon: J. Phys.: Condens. Matter
196 **21** (2009) 145403.
- 197 13) N. R. Keskar and J. R. Chelikowsky: Phys. Rev. B **46** (1992) 1.
- 198 14) F. Liu, S. H. Garofalini, D. King-Smith, and D. Vanderbilt: Phys. Rev. B **49** (1994)
199 12528.
- 200 15) D. R. Hamann: Phys. Rev. Lett. **76** (1996) 660.
- 201 16) Th. Demuth, Y. Jeanvoine, J. Hafner, and J. G. Ángyán: J. Phys.: Condens. Matter
202 **11** (1999) 3833.
- 203 17) M. Catti, B. Civalleri, and P. Ugliengo: J. Chem. Phys. **104** (2000) 7259.
- 204 18) D. M. Christie and J. R. Chelikowsky: Phys. Rev. B **62** (2000) 14703.
- 205 19) M. Sahnoun, C. Daul, R. Khenata, and H. Baltache: Eur. Phys. J. B **45** (2005) 455.
- 206 20) C. Sevik and C. Bulutay: J. Mater. Sci. **42** (2007) 6555.

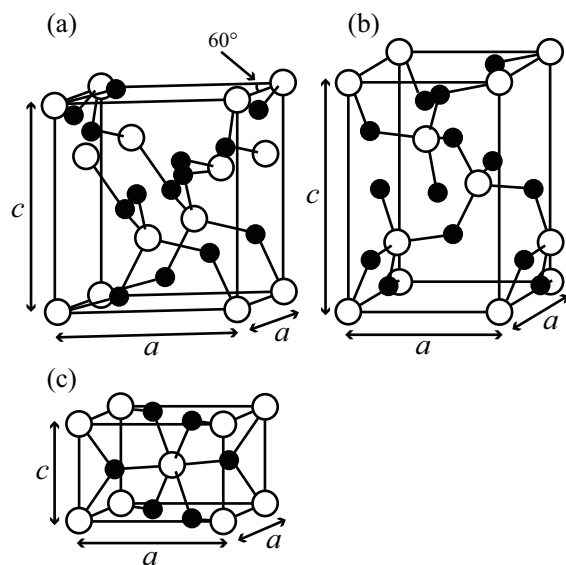
- 207 21) J. P. Perdew and A. Zunger: Phys. Rev. B **23** (1981) 5048.
- 208 22) P. Hohenberg and W. Kohn: Phys. Rev. **136** (1964) B864.
- 209 23) W. Kohn and L. J. Sham: Phys. Rev. **140** (1965) A1133.
- 210 24) J. R. Chelikowsky, N. Troullier, and Y. Saad: Phys. Rev. Lett. **72** (1994) 1240.
- 211 25) J. R. Chelikowsky, N. Troullier, K. Wu, and Y. Saad: Phys. Rev. B **50** (1994) 11355.
- 212 26) K. Hirose, T. Ono, Y. Fujimoto, and S. Tsukamoto: *First-Principles Calculations in*
213 *Real-Space Formalism, Electronic Configurations and Transport Properties of Nanos-*
214 *tructures* (Imperial College, London, 2005).
- 215 27) T. Ono and K. Hirose: Phys. Rev. Lett. **82** (1999) 5016.
- 216 28) T. Ono and K. Hirose: Phys. Rev. B **72** (2005) 085115.
- 217 29) We used the norm-conserving pseudopotentials NCPS97 constructed by K.
218 Kobayashi. See K. Kobayashi: Comput. Mater. Sci. **14** (1999) 72.
- 219 30) N. Troullier and J. L. Martins: Phys. Rev. B **43** (1991) 1993.
- 220 31) L. Kleinman and D. M. Bylander: Phys. Rev. Lett. **48** (1982) 1425.
- 221 32) The difference in the formation energy between the q- and r-GeO₂ phases obtained
222 by our study is larger than that in ref. 18 because only one k -points in the Brillouin
223 zone is used in ref. 18. We confirmed that the total energy of q-GeO₂ deviates by \sim
224 0.28 eV/m.u. depending on the sampling point in the Brillouin zone in the case of
225 one k -point sampling.
- 226 33) R. W. G. Wyckoff: *Crystal Structures* (Wiley, New York, 1965) Vol. 1.
- 227 34) G. S. Smith and P. B. Isaacs: Acta Crystallogr. **17** (1964) 842.
- 228 35) R. M. Hazen and L. W. Finger: J. Phys. Chem. Solids **42** (1981) 143.
- 229 36) J. J. Pluth, J. V. Smith, and J. Faber: J. Appl. Phys. **57** (1985) 1045.
- 230 37) M. Sugiyama, S. Endo, and K. Koto: Mineral. J. **13** (1987) 455.
- 231 38) H. Grimm and B. Dorner: J. Phys. Chem. Solids **36** (1975) 407.
- 232 39) M. O'Keefe and B. G. Hyde: Acta Crystallogr. Sect. B **32** (1976) 2923.
- 233 40) See, for example, A. Molle, Md. N. K. Bhuiyan, G. Tallarida, and M. Fanciulli: Appl.
234 Phys. Lett. **89** (2006) 083504.

Table I. Calculated and experimental lattice constants (unit: Å).

	Present work		Other works			Experiment		
	a	c	a	c	Ref.	a	c	Ref.
q-GeO ₂	4.897	5.636	4.870	5.534	20	4.987	5.652	34
c-GeO ₂	4.818	7.128				4.985	7.070	6
r-GeO ₂	4.418	2.886	4.283	2.782	20	4.397	2.863	35
q-SiO ₂	4.850	5.348	4.883	5.371	20	4.916	5.405	9
c-SiO ₂	4.925	6.828	4.950	6.909	20	4.929	6.847	36
r-SiO ₂	4.147	2.662	4.175	2.662	20	4.180	2.667	37

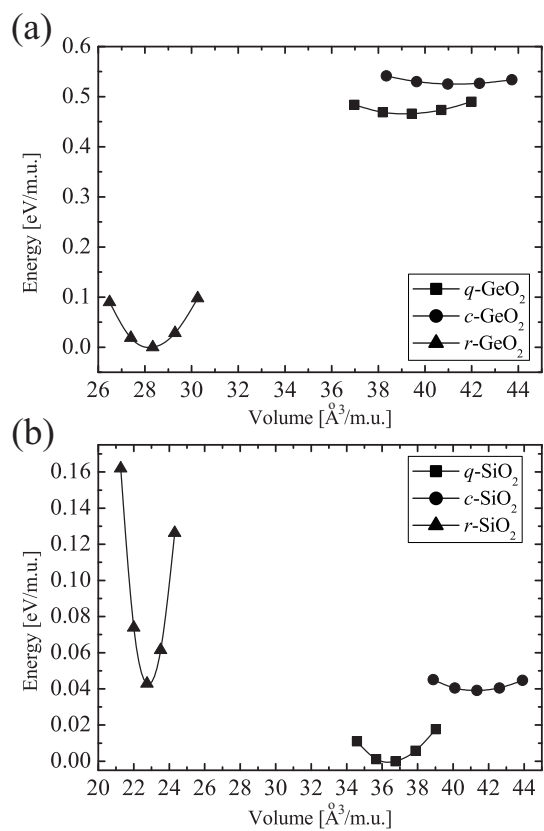
Table II. Bond lengths l_i (in Å), bond angles θ_j , and tilt angles δ (in deg) of GeO₂ and SiO₂ polymorphs. θ_1 , θ_2 , θ_3 , and θ_4 are the O-x-O angles, where x represents a Ge or Si atom. l_i and θ_j are assigned according to the magnitude.

		l_1	l_2	θ_1	θ_2	θ_3	θ_4	δ
q-GeO ₂	Present work	1.763	1.755	114.13	110.69	107.28	105.39	29.66
	Ref. 34	1.741	1.737	113.1	110.4	107.7	106.3	26.54
c-GeO ₂	Present work	1.760	1.760	120.69	111.39	109.95	101.72	35.64
—								
r-GeO ₂	Present work	1.918	1.887	80.25				
	Ref. 35	1.903	1.871	80.2				
q-SiO ₂	Present work	1.608	1.603	110.58	109.37	109.23	108.55	17.85
	Ref. 9	1.614	1.605	110.52	109.24	108.93	108.81	16.37
c-SiO ₂	Present work	1.604	1.603	111.46	110.02	109.01	108.15	25.41
	Ref. 10	1.603	1.603	111.42	109.99	109.03	108.20	23.25
r-SiO ₂	Present work	1.786	1.751	81.02				
	Ref. 37	1.810	1.758	81.35				



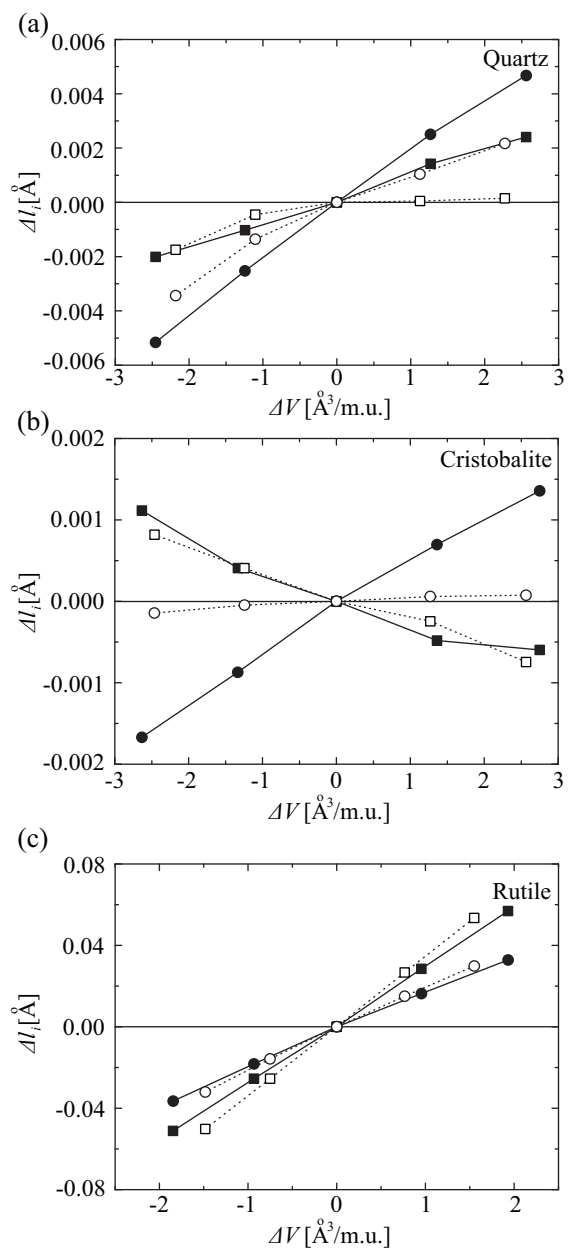
235 **Figure caption**

236 Fig. 1. Unit cells of quartz (a), cristobalite (b), and rutile (c). Black and white circles are O and Ge (Si) atoms, respectively.



237 **Figure captions**

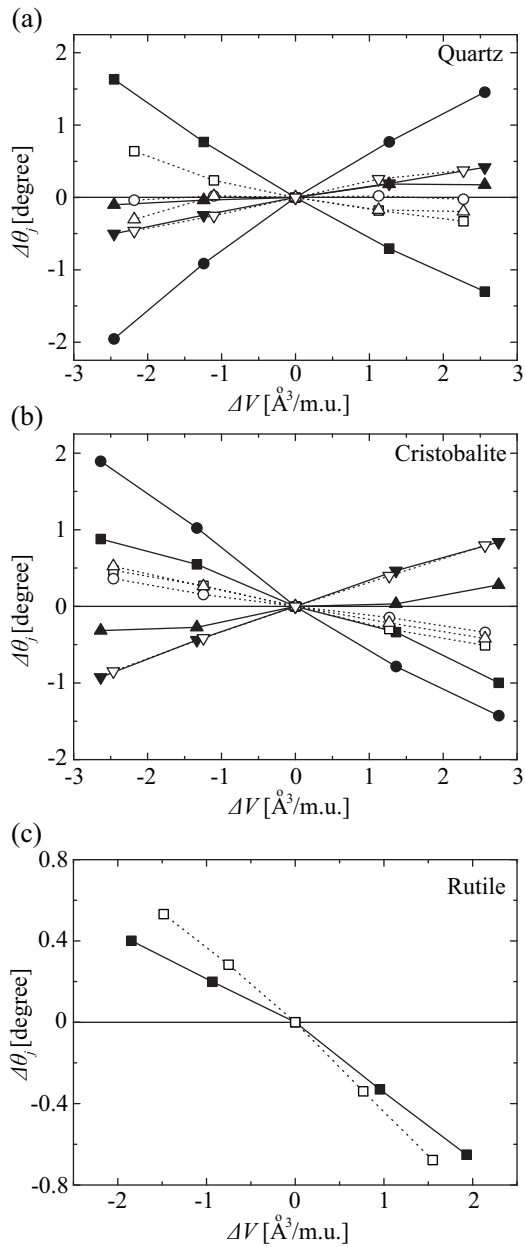
Fig. 2. Total energy per molecular unit (m.u.) as a function of volume for all polymorphs
 238 of GeO₂ (a) and SiO₂ (b). The zero of the energy scale is rutile for GeO₂ and quartz
 for SiO₂.



239 **Figure captions**

Fig. 3. Variations of x-O bond lengths Δl_i in quartz (a), cristobalite (b), and rutile (c) structures from their equilibrium points. x represents a Ge or Si atom. Δl_1 and Δl_2 correspond to squares and circles, respectively. Black (white) symbols are the results of GeO₂ (SiO₂) and lines are only eye guides.

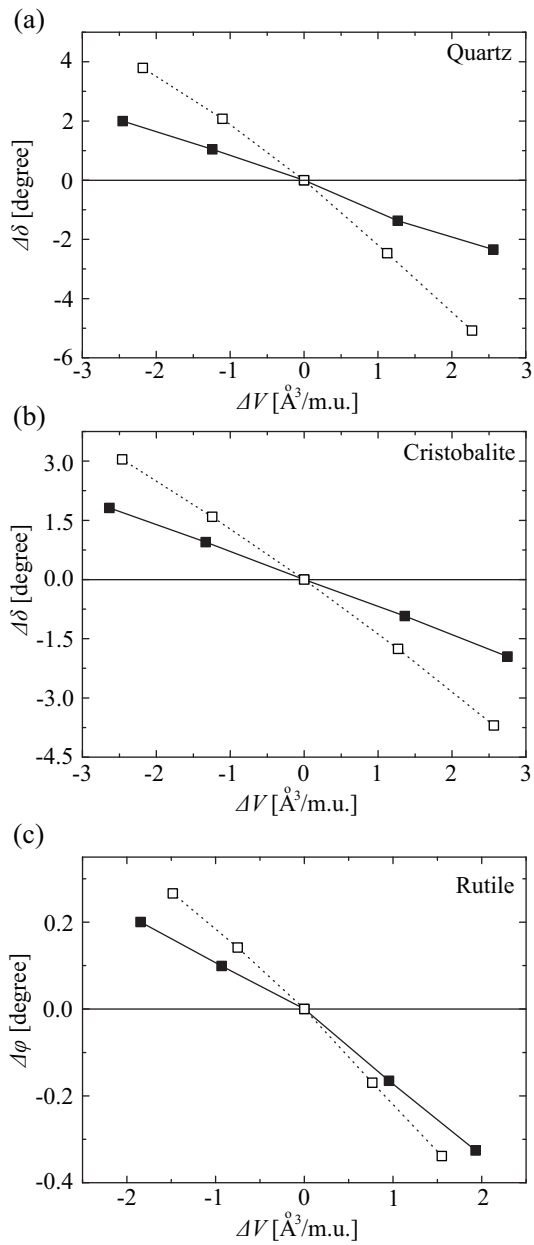
240



241 **Figure captions**

Fig. 4. Variations of O-x-O bond angles $\Delta\theta_j$ in quartz (a), cristobalite (b), and rutile (c) structures from their equilibrium points. x represents a Ge or Si atom. $\Delta\theta_1$, $\Delta\theta_2$, $\Delta\theta_3$, and $\Delta\theta_4$ correspond to squares, circles, upper triangles, and lower triangles, respectively. Black (white) symbols are the results of GeO₂ (SiO₂) and lines are only eye guides.

242



243 **Figure captions**

Fig. 5. Variations of tilt angles $\Delta\delta$ in quartz (a) and cristobalite (b) structures from their equilibrium points. $\Delta\delta$ is related to x-O-x bond angles. Variations of x-O-x bond angles $\Delta\varphi$ in rutile phases from their equilibrium points are shown in (c). x represents a Ge or Si atom. Black (white) symbols are the results of GeO₂ (SiO₂) and lines are only eye guides.

244